MANUFACTURING REQUIREMENTS

Bruce J. Holmes
NASA Langley Research Center
Hampton, Virginia 23665

Clifford J. Obara, Glenn L. Martin,
and Christopher S. Domack
PRC Kentron, Inc.
Hampton, Virginia 23666

SUMMARY

In recent years, natural laminar flow (NLF) has been proven to be achievable on modern smooth airframe surfaces over a range of cruise flight conditions representative of most current business and commuter aircraft. Published waviness and boundary-layer transition measurements on several modern metal and composite airframes have demonstrated the fact that achievable surface waviness is readily compatible with laminar flow requirements. Currently, the principal challenge to the manufacture of NLF-compatible surfaces is two-dimensional roughness in the form of steps and gaps at structural joints. This paper presents results of recent NASA investigations on manufacturing tolerances for NLF surfaces, including results of a flight experiment. Based on recent research, recommendations are given for conservative manufacturing tolerances for waviness and shaped steps.

INTRODUCTION

Many modern metal and composite airframe manufacturing techniques can provide surface smoothness which is compatible with natural laminar flow (NLF) requirements (ref. 1). Specifically, this has been shown in flight investigations over a range of free-stream conditions including Mach numbers up to 0.7, chord Reynolds numbers up to about 30 million, and transition Reynolds numbers up to about 14 million. Surface smoothness requirements relate to waviness, to two-dimensional steps and gaps, and to three-dimensional roughness elements. The recent flight experiments were conducted on flush-riveted thin aluminum skins, integrally stiffened milled thick aluminum skins, bonded thin aluminum skins, and composite surfaces. The most important conclusion concerning manufacturing to be drawn from these experiences is that the waviness of the surfaces in the tests met the NLF criterion for the free-stream conditions flown. However, in addition to waviness, an equally important consideration is manufacturing roughness of the surface in the form of steps and gaps perpendicular to the free stream. While much work has been done in the past, many unknowns still exist concerning the influences of wing sweep, compressibility, and shapes of steps or gaps on manufacturing tolerances for laminar flow surfaces. Even less information is available concerning NLF requirements related to practical three-dimensional roughness elements such as flush screw head slots and incorrectly installed flush rivets.

The principal challenge to the design and manufacture of laminar flow surfaces today appears to be in the

installation of leading-edge panels on wings, nacelle, and empennage surfaces. Another similar challenge is in the installation of access panels, doors, windows, and the like on fuselage noses and engine nacelles, where laminar flow may be desired. These surface discontinuities appear to be unavoidable for typical current aircraft; the challenge is, "Can laminar flow be maintained over these discontinuities?" Figure 1 illustrates the drag reduction benefits available from laminar flow on various airframe components on a medium-sized subsonic business jet. These are not integrated benefits, but rather the benefits of adding laminar flow to a fixed airframe geometry. Figure 1 shows that significant fuel efficiency improvements of the order of 25 percent are possible. Such improvements are strong motivation for understanding how to achieve laminar flow over surface discontinuities.

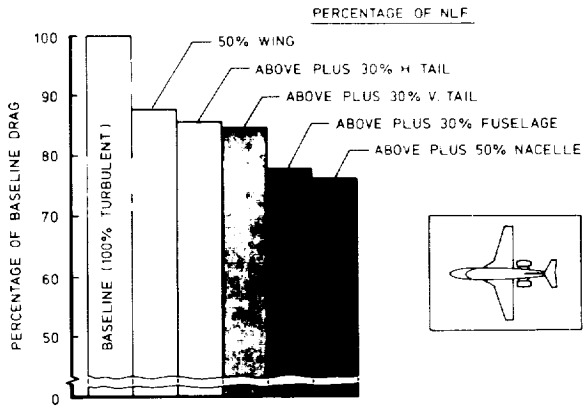

Figure 1. Predicted drag benefits of laminar flow on a subsonic business jet.

The purpose of this paper is to present results and analyses of recent NASA Langley research on manufacturing tolerances for waviness and shaped steps on NLF surfaces for subsonic aircraft. No treatment is given herein of tolerances for three-dimensional roughness effects. The paper includes a review and discussion of past manufacturing tolerances research.

SYMBOLS

C_{D_o}	profile drag coefficient
C_ℓ	section lift coefficient
C_p	pressure coefficient
c	local chord, in.
h	step height, gap width, or double amplitude wave length, in. or ft
h'	height of a bulge above nominal surface, in. or ft
H	altitude, ft
M	Mach number
n	logarithmic exponent of Tollmien-Schlichting amplitude ratio
R'	free-stream unit Reynolds number, ft^{-1}
R_c	chord Reynolds number
R_h	roughness height Reynolds number
s_t	surface length from stagnation to transition, ft
u_e	boundary-layer edge velocity, ft/sec
U_∞	free-stream velocity, ft/sec
x	longitudinal dimension, ft
θ	boundary-layer momentum thickness, in.
ν	kinematic viscosity, ft^2/sec
Λ	wing leading-edge sweep angle, deg
Λ_s	angle between ridge of a step and the free stream
λ	length of wave, bulge, ridge, or hollow, in.

Subscripts:

crit critical

max maximum

∞ free stream

LAMINAR BOUNDARY-LAYER TOLERANCES TO SURFACE IMPERFECTIONS

Existing criteria for NLF surfaces deal with waviness and with both two- and three-dimensional roughness. Each of these types of surface imperfections can cause transition by different mechanisms in the boundary layer. The definition of critical height for waviness or roughness is related to the mechanism by which transition is affected. The mechanisms of most practical interest include laminar separation, amplification of Tollmien-Schlichting (T-S) waves, amplification of crossflow vorticity, and interactions between any of these mechanisms. In addition, free-stream turbulence and acoustic disturbances may interact with these mechanisms to influence critical waviness and roughness heights. Criteria exist only for critical waviness and roughness which cause either laminar separation or amplification of T-S waves. No criteria exist which fully address surface-imperfection-induced transition related to crossflow amplification on swept wings or interactions between the various transition mechanisms and free-stream disturbances.

The following definitions appear in the literature and are useful for the present discussion. Critical waviness height to length ratio (h/λ) and critical step height or gap width can be defined as those which produce transition forward of the location where it would occur in the absence of the surface imperfection. Experimentally, premature transition was identified in past work as the first appearance of turbulent bursts downstream of either a waviness or roughness surface imperfection. This is the definition used in references 2 to 5 to establish critical conditions for surface imperfections.

For most common applications in two-dimensional flows, this definition physically relates to the viscous amplification of T-S waves or to (Rayleigh's) inflectional instability growth over a laminar separation bubble. Figure 2 illustrates possible effects of a given two-dimensional surface imperfection on transition. A subcritical condition exists when transition is unaffected by the disturbance (top of figure). The middle of figure 2 illustrates the critical condition at which transition just begins to be affected by the disturbance. In the extreme, a surface imperfection could cause sufficiently rapid T-S wave amplification for transition to occur very near the wave itself, as illustrated at the bottom of figure 2.

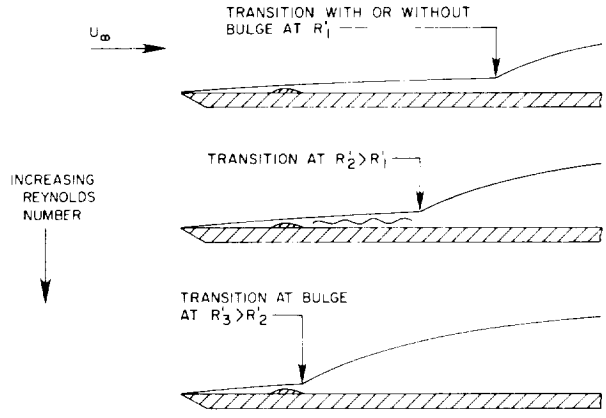

Figure 2. Effects of two-dimensional surface imperfection on laminar flow.

Another limiting condition of practical interest is the occurrence of transition at the surface imperfection caused by the inflectional instability in the free shear layer over the laminar separation bubble formed there. Using flight data (from ref. 6), figure 3 illustrates the predicted local increase in growth rate of T-S instability caused by a surface wave. The surface wave tested was h = 0.010 in. and λ = 2.5 in.; the effects of this wave on the pressure distribution between 0.10 < x/c < 0.13 and on maximum T-S amplitude ratios are apparent in the figure. In the adverse pressure gradient of the wave, n_{max} is seen to grow from about 1 to near 4. Elsewhere, in favorable pressure gradients, the rate of growth of the T-S disturbance is damped.

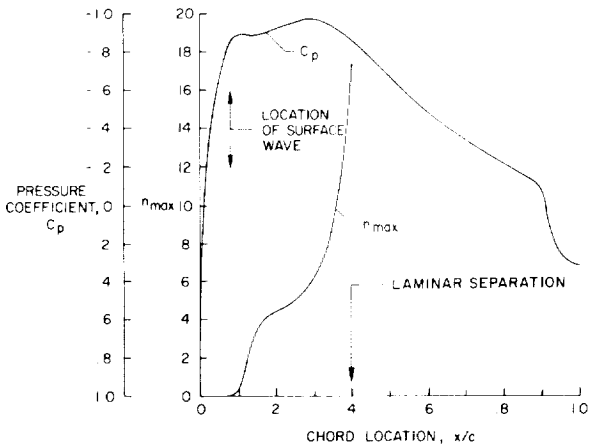

Figure 3. Tollmien-Schlichting instability growth in the presence of a surface wave.

From Schlichting (ref. 7), the laminar boundary layer will separate for $(\theta^2/\nu)(du_e/dx) < -0.1567$ where θ is the boundary-layer momentum thickness, ν is the local kinematic viscosity, and u_e is the local potential flow velocity. Calculation of values of $(\theta^2/\nu)(du_e/dx)$ for both Fage's and Carmichael's surface imperfections indicates that the critical value for laminar separation was exceeded at most of the test conditions for those studies. For example, at the conditions shown in figure 4 (from Fage), $(\theta^2/\nu)(du_e/dx) = -0.19$. Similar results occur for analysis of Carmichael's data from

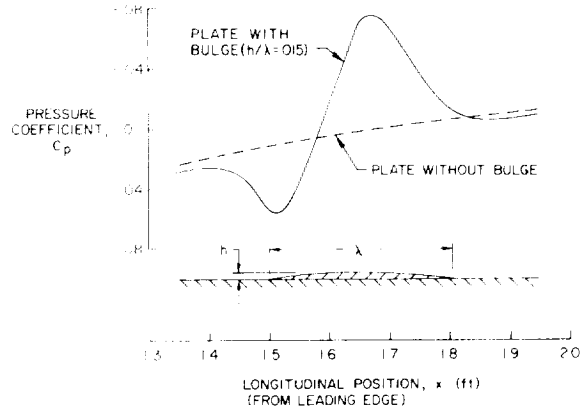

Figure 4. Pressure distributions over a bulge, from Fage (ref. 2).

reference 3. It appears then that for many of the critical surface imperfections tested by Fage and Carmichael, laminar separation at the imperfection was present. Thus, the mechanism for forward movement of transition due to a surface imperfection could involve both the effect of local adverse pressure gradient on T-S amplification and the effect of Rayleigh's inflectional instability.

CRITERIA FOR WAVINESS

The classical research by Fage (ref. 2) provided criteria for critical height of 2-D bulges, ridges, and hollows in incompressible 2-D boundary layers. His shapes, as illustrated in figure 5, do not accurately represent many of the surface imperfections observed on modern airframe surfaces. However, the pressure disturbances over Fage's bulges and hollows do simulate

those which will occur over sinusoidal waves. In spite of these limitations, Fage's experiments did provide an understanding of some of the mechanisms associated with transition over these imperfections.

The research of Carmichael (refs. 3 to 5) provided the basis for the existing criterion on allowable waviness for both swept and unswept wing surfaces. Carmichael's criterion applies to single and multiple bulges or sinusoidal waves above the nominal surface which produce sinusoidal-shaped disturbances in the pressure distribution. As previously discussed, transition in Carmichael's surface waviness experiments may have been related to either laminar separation or to amplified Tollmien-Schlichting wave growth. This T-S amplification over a surface wave results from the decreased boundary-layer stability in the adverse pressure gradient on the aft side of a wave, but may also be influenced by resonance between the critical T-S frequency and the surface waviness frequency (wavelength of multiple, closely spaced waves) (refs. 3 and 8). Carmichael's investigations at least partially included the influences of compressibility, boundary-layer stabilization by suction and pressure gradient, multiple waves, and wing sweep.

Compressibility influences allowable waviness in two ways. First, compressibility favorably increases the damping of growth rates for T-S waves. The second unfavorable effect results from the increased pressure peak amplitude over a wave due to compressibility. It is not clear which effect dominates.

With wing sweep, Carmichael and Pfenninger observed a slight reduction in allowable waviness (ref. 5). Furthermore, a slightly greater reduction in allowable (h/λ) was observed for multiple waves on a swept wing than for multiple waves on an unswept wing. This might be expected to result from the interaction between the T-S instability growth in the deceleration on the backside of the wave and the crossflow instability growth due to the spanwise pressure gradient. Carmichael defined a critical wave as the minimum (h/λ) which prevents the attainment of laminar flow to the trailing edge under boundary-layer stabilization using moderate suction. On a non-suction wing, the criterion applies for waves in regions of boundary-layer stabilization using a favorable pressure gradient (flow acceleration). The criterion was based on experimental results for waves located more than 25 percent of the chord downstream of the leading edge. Thus for waves located in very highly accelerated flows closer to the leading edge, the criterion may underpredict allowable waviness. Conversely, the criterion would overpredict the allowable waviness in a region of unaccelerated flow; for this case, the criterion provided by Fage (ref. 2) from his flat plate experiments would provide better information. Fage's criterion is given by

$$\frac{h'}{s_t} = 9 \times 10^6 \left[\frac{u_e s_t}{\nu}\right]^{-3/2} \left[\frac{\lambda}{s_t}\right]^{1/2} \qquad (1)$$

which can be more conveniently written

$$\frac{h'}{\lambda} = 9 \times 10^6 \left[\frac{u_e s_t}{\nu}\right]^{-3/2} \left[\frac{s_t}{\lambda}\right]^{1/2} \qquad (2)$$

where h' is the height of a bulge in feet above the nominal surface, λ is the length of the bulge in feet, s_t is

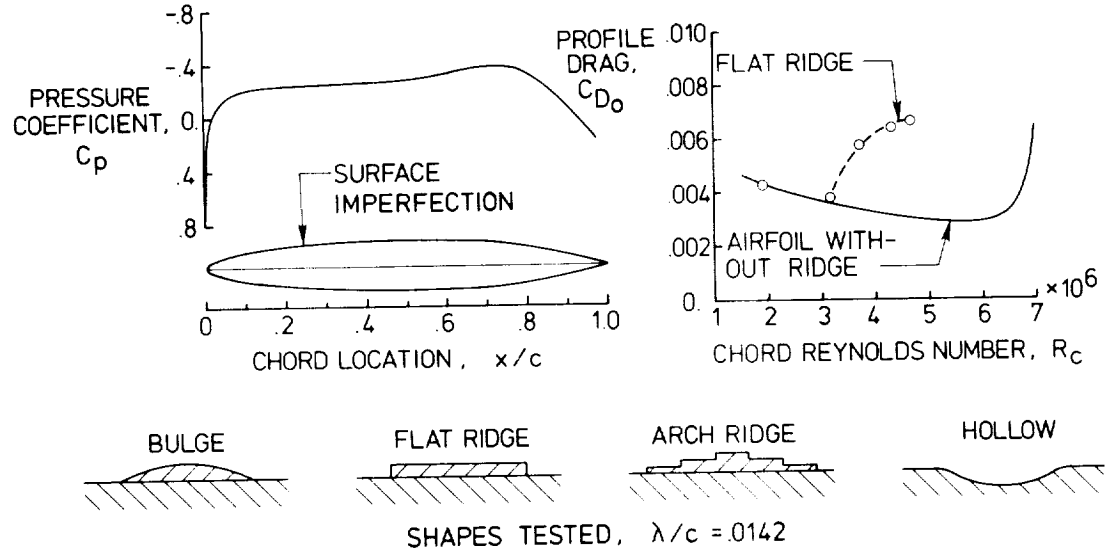

Figure 5. Shapes of two-dimensional surface imperfections tested by Fage (ref. 2).

the surface length to transition in feet, u_e is the boundary-layer edge velocity in feet per second at the location of the center of the bulge for the undistorted surface, and ν is the kinematic viscosity. Using local C_p and free-stream velocity, u_e can be determined directly for use in equation (2). Fage's work covered a range of transition Reynolds numbers from 1 x 10^6 to 3.5 x 10^6 and did not include any effects of compressibility or sweep.

Carmichael's waviness criterion is given as

$$\frac{h}{\lambda} = \left(\frac{59000\, c \cos^2 \Lambda}{\lambda\, R_c^{1.5}}\right)^{0.5} \qquad (3)$$

where h is the double-amplitude wave height in inches, λ is the wavelength in inches, c is the streamwise wing chord in inches, Λ is the wing leading-edge sweep, and R_c is the chord Reynolds number based on chord length and airspeed in the free-stream direction. Note the difference in the definition of wave heights, h and h', used in equations (2) and (3). For waves which have their peaks and valleys aligned in the chordwise direction, the recommendation of reference 9 is to double the value of h/λ from equation (3).

The dial indicator mounted on a 2-in. base has been used for decades to document waviness. On a swept wing, both h and λ are most appropriately measured normal to the leading edge since most of the aircraft structure which is responsible for waviness is oriented this way. This practice will only slightly and conservatively affect the measured surface wave height to length ratios for wings of moderate sweep (as compared to measuring waviness in the free-stream direction).

For conservatism, Carmichael proposed that the value of (h/λ) from equation (3) be multiplied by 1/3 to estimate tolerances for multiple waves. However, this multiple waviness criterion was developed using closely spaced waves and does not address any effects due to widely spaced waves. As previously discussed, closely spaced waves may have a T-S resonance effect

which might be less likely to occur for widely spaced waves. Furthermore, the wind-tunnel and flight experimental results used to develop the factor of 1/3 actually varied over a range from 1/3 to 3/4, with the flight values being typically greater than the wind-tunnel values. Thus, some uncertainty exists concerning a realistic method for figuring the effect of multiple waves on the allowable (h/λ). Carmichael (ref. 4) notes that "...if the wing design can be accomplished such that waviness is reduced to a low value, then a few waves at major structural points could be permitted with a somewhat larger tolerance than (that calculated using the 1/3 factor)." As discussed in reference 10, most waviness observed on modern airframe surfaces typically consists of only one or two waves, widely spaced, at major structural joints. This observation was also made for very stiff skins (on missiles and on certain supersonic airplanes) as early as 1959. (See ref. 11.)

Consistently in recent flight experiments (ref. 1), the measured aircraft surface waviness was better than required as calculated by Carmichael's criterion, using the single-wave assumption. A selected number of these comparisons are illustrated in figure 6. All but one of the waves shown are significantly smaller than allowable. Since the allowable waviness values were calculated for the low altitudes and high speeds of the flight experiments, the allowable waviness at lower Reynolds numbers for typical cruise conditions for all of the airplanes will be even larger than shown. During the flight experiments on these airplanes at the chord Reynolds numbers indicated in figure 6, no transition due to waviness was observed. Thus, a conservative value for allowable waviness on unswept ($\Lambda < 15°$) NLF wings can be determined using equation (3) for a single wave. Use of a single-wave assumption will result in larger allowable wave heights which are easier and less costly to achieve in production.

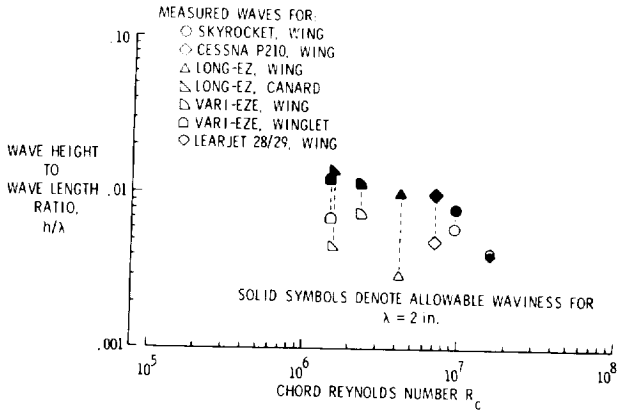

Figure 6. Comparisons of allowable and actual waviness measured on airplanes used for NLF flight experiments.

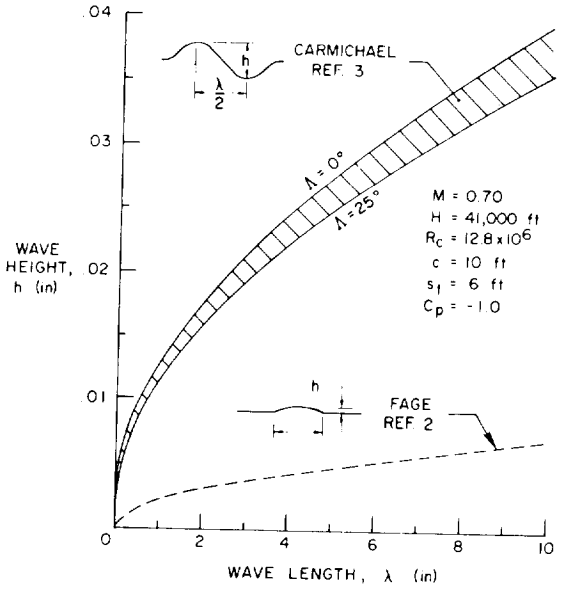

Figure 7. Allowable waviness for a business jet at cruise conditions. From Fage (ref. 2) and Carmichael (ref. 3).

Figure 7 presents examples of allowable waviness for free-stream conditions representative of a high performance business airplane flying at Mach 0.7 at 41,000 ft. The chart shows allowable waviness using both equations (2) and (3). Using Carmichael's criterion (eq. (3)), the effect of sweep on allowable waviness is seen to be on the order of 10 percent. These calculations show that with a wavelength of 6 in., the allowable wave height is 0.025 in. on a 25° swept wing, with a favorable pressure gradient. Such a manufacturing tolerance for waviness is within the capabilities of modern airframe manufacturing methods. Were this same 6-in. wave in a region of unaccelerated flow, the allowable height would be about 0.010 in. This calculation assumes it is reasonable to relate h to h' by a factor of 2; that is, an allowable double amplitude wave height may be estimated using 2 x h' in equation (2) for comparisons with h in equation (3).

The dashed line for Fage's criterion in figure 7 is presented with the caution that it has never been verified for compressible flows. The figure shows the effect of an unaccelerated flow (Fage's criterion) on reducing the allowable waviness significantly compared to allowable waviness in an accelerated flow (Carmichael's criterion). This result illustrates the dominant effect of pressure gradient on waviness tolerances. The reason for this effect is explained by the dominant effect of pressure gradient on boundary velocity profiles and, hence, on T-S stability.

CRITERIA FOR STEPS AND GAPS

A potentially misleading conclusion from Fage (ref. 2) was that shape did not affect the critical size of the surface imperfection. This conclusion resulted, at least in part, from the particular shapes tested by Fage. (See fig. 5.) In the case of his ridges, each shape produced a laminar separation region at the front of the ridge and a second laminar separation at the aft-facing step on the downstream edge of the ridge. Transition behind Fage's ridges could have been dominated by the inflectional instability growth over these two separated flow regions. For modern airframe surfaces, the simple forward-facing step, aft-facing step, or gap (perpendicular to the free stream) is of more practical interest. Figure 8 shows the characteristics of laminar separation over such a step.

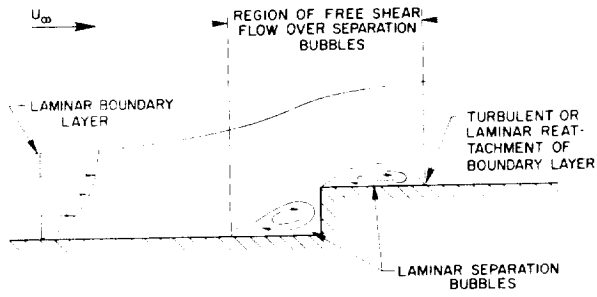

Figure 8. Characteristics of laminar separation over a step.

The past work on criteria for step and gap tolerances came from the X-21 experiments (ref. 9). The literature does not state what definition was used to determine critical Reynolds numbers for these surface imperfections. However, according to Dr. Werner Pfenninger, who conducted wind-tunnel experiments to develop these criteria, the critical step height Reynolds number was established based on the conditions where the first turbulent bursts occurred far downstream from the surface imperfection. Thus, these criteria were developed in a manner

consistent with that for the waviness criteria. The critical Reynolds number $R_{h,crit} = (U_\infty/\nu)\, h$ is determined by free-stream airspeed (U_∞), kinematic viscosity, and the height of the step or length of the gap (h). The shapes and critical Reynolds numbers for which tolerances were established in the X-21 experiments are illustrated in figure 9.

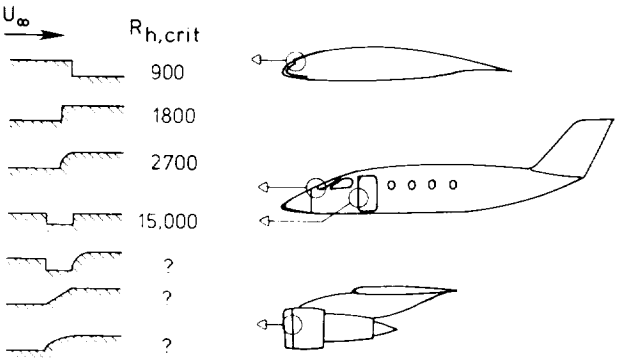

Figure 9. Examples of surface imperfections and tolerances for NLF surfaces.

In addition, figure 9 presents information from recent NASA investigations on the influence of rounded steps on critical Reynolds numbers. For three of the illustrated surface imperfection shapes (indicated by question marks), no criteria exist. The recent NASA flight experiments on shaped steps were conducted on an NLF glove installed on a T-34C airplane. The results are summarized in the following section. Previous flight transition experiments on this glove are described in reference 6.

These recent NASA experiments illustrate (in contrast to Fage's experiments) that shape of the surface imperfection influences the allowable height. The reason for the difference in conclusions of Fage and the recent NASA experiments has to do with sensitivity of the laminar boundary layer to inflectional instability growth over a laminar separation region. In the case of the present experiments, the boundary layer was subjected to smaller regions of laminar separation than in Fage's experiments. This difference occurred because in the NASA experiments, the rounded shape of the step reduced the length of the region of laminar separation over the step; thus, the inflectional instability growth was reduced. Critical step heights may be larger for steps with shapes which reduce the length of the region of laminar separation.

FORWARD-FACING STEP FLIGHT EXPERIMENTS

The forward-facing step was simulated for the NASA flights using a cellulose acetate sheet attached to the lower surface of the glove with double-sided adhesive tape. The thickness of the sheet tested was 0.020 in.; the addition of the adhesive tape produced a total step height of 0.027 in. The sheet had two different leading-edge profiles (see fig. 10); one was a

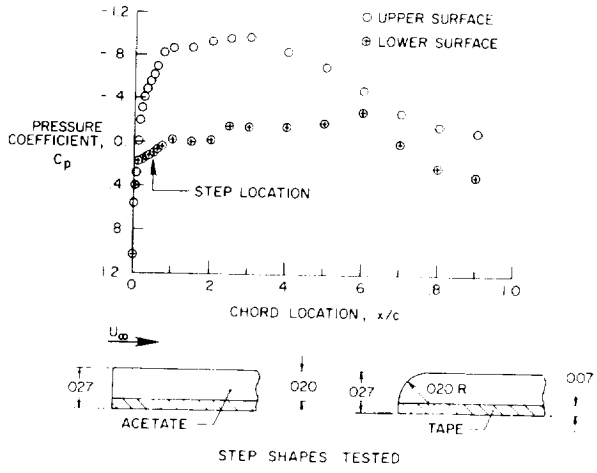

Figure 10. Forward-facing step shapes tested in flight on an NLF glove, $R' = 1.95 \times 10^6$ ft^{-1}. (Dimensions on sketch are in inches.)

square step, the other a rounded step with a 0.020-in. radius. The testing was done with the sheet positioned such that the step was located at the 5-percent chord location on the lower surface. The lower surface pressure distribution at the test condition was only slightly favorable (accelerating) as shown in figure 10. Determination of critical step height Reynolds number for the square and rounded steps was made by flying both step shapes of equal height on one flight and by using sublimating chemicals to detect transition. A flight condition was chosen to provide a step height Reynolds number which would significantly exceed the critical value of 1800 (from ref. 9) for a square forward-facing step. The condition flown resulted in an R_h of 2720, thus exceeding 1800 by more than 50 percent. At this condition, transition occurred at the square step as expected. For the rounded step, on the other hand, transition occurred far downstream from the step (about 2 ft) as illustrated in figure 11.

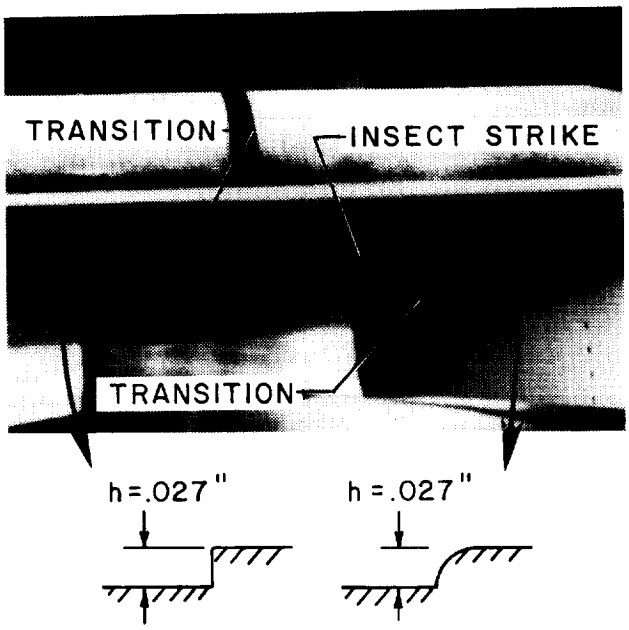

Figure 11. Transition visualization on shaped forward-facing step on T-34C NLF glove flight experiments.

These data establish a conservative value of $R_{h,crit} = 2700$ for a rounded forward-facing step, close to the leading edge, on an unswept wing, with a radius approximately equal to the step height.

Additional flight experiments were conducted to simulate both forward- and aft-facing steps at several sweep angles. The sweep angle in this context is the angle between the ridge of the step and the free stream. Acetate sheets were attached to the upper surface of the T-34C glove in a fashion similar to the previous tests. The purpose of these experiments was to develop a technique for installation of large thin films carrying flush instrumentation (e.g., hot-film transition sensors) on swept airplane wings for NLF flight experiments. These experiments were designed to crudely simulate the flow which a spanwise facing step would see on a swept wing. On an actual swept lifting surface, the presence of crossflow vorticity would very likely produce smaller critical step sizes. The shape of the steps was varied until the step no longer caused boundary-layer transition. The pressure distribution for these tests was similar to that which appears on the upper surface in figure 10. The results are presented in figures 12 and 13. At a step height of 0.0215 in. and a sweep angle of 73°, it can be seen in

C-3

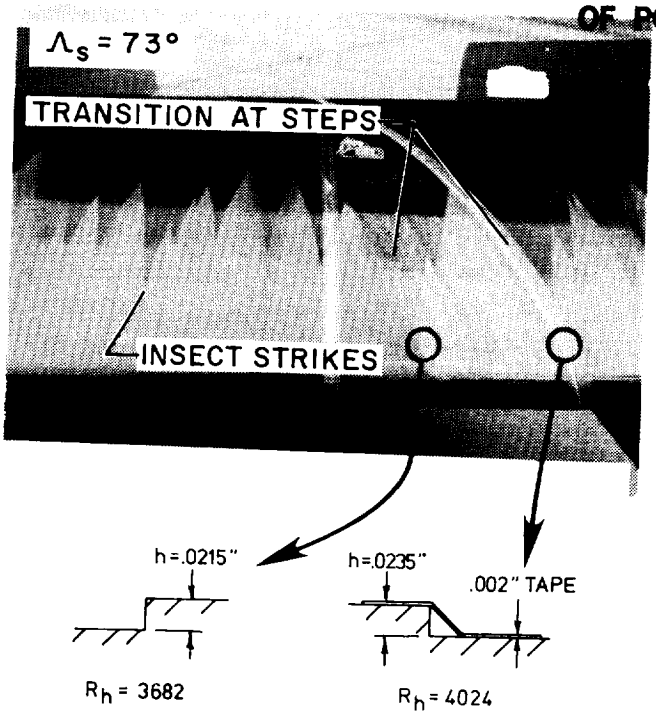

Figure 12. Transition visualization on swept shaped steps on T-34C NLF glove flight experiments.

figure 12 that both the forward-facing square step and the aft-facing ramp step caused transition. Figure 13 shows the modified step shapes that did not cause boundary-layer transition at step sweep angles (Λ_s) of 73° and 45°. The step height Reynolds numbers for these two steps were R_h = 4024 and 4110, for the forward ramp step and the aft ramp step, respectively. These values of R_h can be used as a guide to size allowable forward- and aft-facing steps with up to 45° of step sweep in a region of accelerated two-dimensional flow, with steps shaped as shown in figure 13.

For one set of free-stream conditions representative of a high performance business airplane, figure 14 illustrates allowable step heights and gap widths for a range of cruise altitudes. The strong beneficial effect of higher altitudes on allowable step heights and gap widths is readily apparent. The increases in tolerances with increased altitude result directly from the decrease in unit Reynolds number. As the unit Reynolds number decreases, the length of the laminar separation regions associated with the steps decreases, reducing the growth of the inflectional instability and increasing the allowable step height.

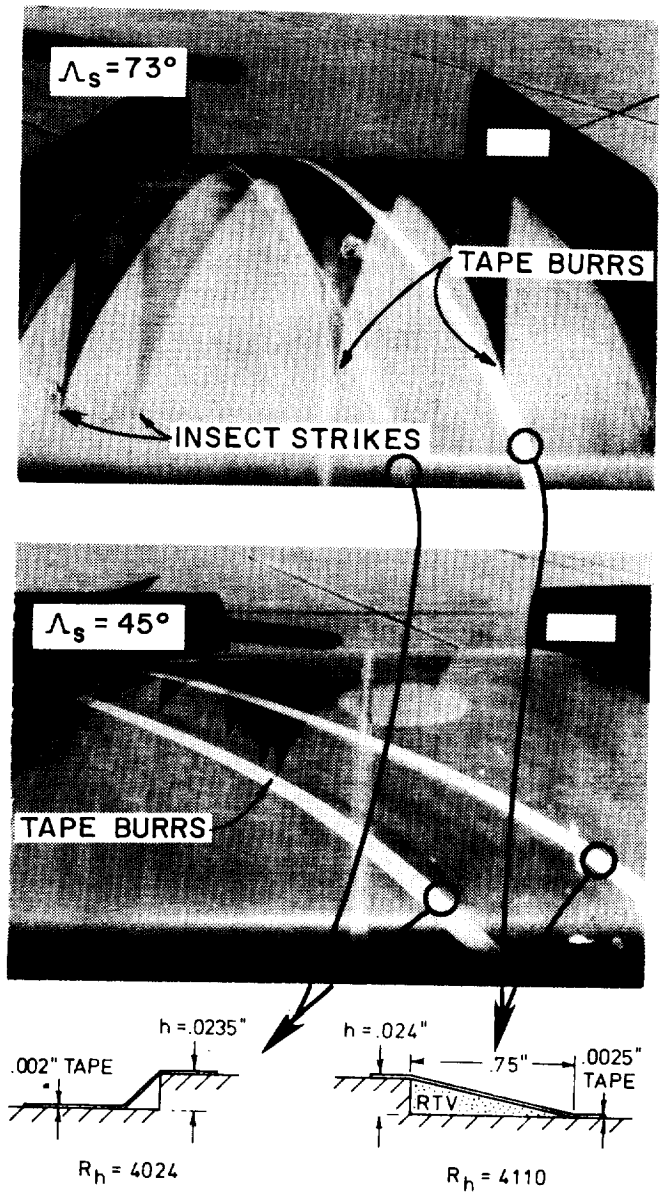

Figure 13. Transition visualization on swept shaped steps on T-34C NLF glove flight experiments.

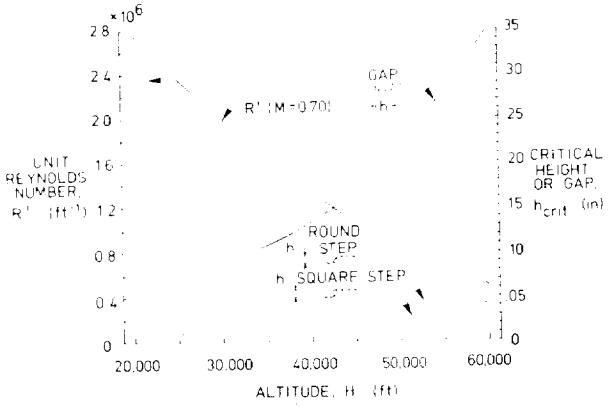

Figure 14. Allowable step heights and gap widths for a range of cruise altitudes at M = 0.7.

CONCLUDING REMARKS

A review of past work on roughness and waviness manufacturing tolerances and comparisons with more recent experiments provided the following conclusions:

1. On modern airframe surfaces where large waves typically occur only at major structural joints, the assumption of multiple waves for use of Carmichael's waviness criterion is too conservative. Based on recent flight experiences with modern airframes, it is recommended that Carmichael's criterion be used with the single-wave assumption.

2. In contrast to Fage's conclusion concerning the unimportance of the shape of a two-dimensional step in a laminar boundary layer, it has been demonstrated experimentally that shape has a significant effect on critical Reynolds numbers.

3. For a forward-facing rounded step, close to the leading edge, with a radius approximately equal to the step height, a conservative value for $R_{h,crit}$ of 2700 is indicated. This value is more than a 50-percent increase over the critical step height Reynolds number for a forward-facing square step.

4. For steps with up to 45° of sweep relative to the free stream in two-dimensional flows, step height Reynolds numbers of 4000 and 4100 can be used as a guide to size foward- and aft-facing steps, respectively. These values apply to swept forward-facing steps with rounded corners and to swept aft-facing ramp steps.

REFERENCES

1. Holmes, B.J., Obara, C.J., and Yip, L.P., "Natural Laminar Flow FLight Experiments on Modern Airplane Surfaces," NASA TP 2256,1984.

2. Fage, A., "The Smallest Size of Spanwise Surface Corrugation Which Affects Boundary Layer Transition on an Airfoil," R&M No. 2120, Brit. A.R.C., 1943.

3. Carmichael, B.H., Whites, R.C., and Pfenninger, W., "Low Drag Boundary Layer Suction Experiments in Flight on the Wing Glove of an F-94A Airplane," Northrop Aircraft Inc. Rep. No. NAI-57-1163 (BLC-101), 1957.

4. Carmichael, B.H., "Surface Waviness Criteria for Swept and Unswept Laminar Suction Wings," Norair Rep. No. NOR-59-438 (BLC-123), 1959.

5. Carmichael, B.H., and Pfenninger, W., "Surface Imperfection Experiments on a Swept Laminar Suction Wing," Norair Rep. No. NOR-59-454 (BLC-124), 1959.

6. Obara, C.J., and Holmes, B.J., "Flight Measured Laminar Boundary-Layer Transition Phenomena Including Stability Theory Analysis," NASA TP 2417, 1985.

7. Schlichting, H., Boundary Layer Theory, McGraw-Hill, 7th ed., 1979.

8. Spence, D.A., and Randall, D.G., "The Influence of Surface Waves on the Stability of a Laminar Boundary Layer With Uniform Suction," A.R.C. C.P. No. 161 (15.916), T.N. No. AERO 2241, 1953.

9. Anon, "Final Report on LFC Aircraft Design Data Laminar Flow Control Demonstration Program," NOR 67-136 (Contract AF 33(657)-13930), Northrop Corp., June 1967. (Available from DTIC as AD 819 317).

10. Holmes, B.J., "Progress in Natural Laminar Flow Research," AIAA Paper 84-2222, 1984.

11. Stall, C.G., and Pfenninger, W., "Present Status of Production Aircraft Surface Waviness at Norair. Norair Rep. No. NOR-59-444 (BLC-126), 1959.